
Princeton Plasma Physics Laboratory

PPPL-

PPPL-



Prepared for the U.S. Department of Energy under Contract DE-AC02-09CH11466.

Princeton Plasma Physics Laboratory

Report Disclaimers

Full Legal Disclaimer

This report was prepared as an account of work sponsored by an agency of the United States Government. Neither the United States Government nor any agency thereof, nor any of their employees, nor any of their contractors, subcontractors or their employees, makes any warranty, express or implied, or assumes any legal liability or responsibility for the accuracy, completeness, or any third party's use or the results of such use of any information, apparatus, product, or process disclosed, or represents that its use would not infringe privately owned rights. Reference herein to any specific commercial product, process, or service by trade name, trademark, manufacturer, or otherwise, does not necessarily constitute or imply its endorsement, recommendation, or favoring by the United States Government or any agency thereof or its contractors or subcontractors. The views and opinions of authors expressed herein do not necessarily state or reflect those of the United States Government or any agency thereof.

Trademark Disclaimer

Reference herein to any specific commercial product, process, or service by trade name, trademark, manufacturer, or otherwise, does not necessarily constitute or imply its endorsement, recommendation, or favoring by the United States Government or any agency thereof or its contractors or subcontractors.

PPPL Report Availability

Princeton Plasma Physics Laboratory:

<http://www.pppl.gov/techreports.cfm>

Office of Scientific and Technical Information (OSTI):

<http://www.osti.gov/bridge>

Related Links:

[U.S. Department of Energy](#)

[Office of Scientific and Technical Information](#)

[Fusion Links](#)

Comment on Li pellet conditioning in TFTR

R. V. Budny

Princeton Plasma Physics Laboratory, Princeton, NJ 08543

(Dated: May 24, 2011)

Li pellet conditioning in TFTR results in a reduction of the edge electron density which allows increased neutral beam penetration, central heating, and fueling. Consequently the temperature profiles became more peaked with higher central T_i , T_e , and neutron emission rates.

PACS numbers: 07.05.Tp, 52.55.Fa

DOE Copyright Terms: "Notice: This manuscript has been authored by Princeton University under Contract Number DE-AC02-09CH11466 with the U.S. Department of Energy. The publisher, by accepting the article for publication acknowledges, that the United States Government retains a non-exclusive, paid-up, irrevocable, world-wide license to publish or reproduce the published form of this manuscript, or allow others to do so, for United States Government purposes."

Wall conditioning is helpful for achieving high plasma performance in tokamaks as measured by high central temperatures, confinement times, and neutron emission. These beneficial effects result from reducing influx from the walls and lowering impurity levels in the core plasma.

One of the wall conditioning techniques is use of Li to coat the walls. There is a renewed interest in studying Li in various fusion test devices [1]. One technique for introducing Li is via pellet injection. This was pioneered in ALCATOR-CMOD where it was first used for impurity transport studies. Li pellet wall conditioning was tried in ALCATOR-CMOD Ohmic H-modes without a big effect except for reduction in H-mode threshold [2]. Li pellet wall conditioning was also tried in ALCATOR-CMOD with ICRF heated shots with peaked density profiles [3]. Enhanced energy confinement and fusion reactivity were seen.

Various conditioning techniques were used in TFTR. The technique which injected the highest amount of Li was injecting an aerosol from laser ablation of Li (DOLLOP) [4]. Li pellet injection was also used extensively in TFTR. Strong improvements in performance were seen. [5]. Typically small ≈ 3 mg pellets were injected before or after the high power phase of the plasma discharge. This paper discusses analysis of a series of TFTR shots using this technique.

The shots studied here were a series of five well diagnosed TFTR shots with Li pellet injection. They showed rapid changes from poorly conditioned to well conditioned supershots. The shots had a flat top current of 2.5 MA and toroidal field of 5.1 T. Deuterium was the bulk hydrogenic species. Traces of hydrogen and tritium from recycling were also present. The shots were heated by D neutral beam injection (NBI) from 3.5 to 4.3 s. The first four had 19.0 MW injected and the fifth had 24.8 MW.

TRANSP analysis [6] was redone to incorporate several improvements recently added to the code. These include the ADAS atomic cross section data [7, 8] which is more up-to-date than the Oak Ridge “Red Book” data used in TRANSP during the TFTR experimental campaign. Also the TEQ equilibrium solver [9] now in TRANSP gives more accurate numerical solutions to the Grad-Shafranov equations compared to the VMEC solver. Neither of these improvements had significant changes in the TRANSP results. The accuracy of the TRANSP analysis modeling is indicated by the the accuracy simulating the neutron emission rate. A comparison of these for the first shot of the series is shown in [Fig. 1](#).

Li pellets were fired into the shots after, and in all but the first shot before the beam heating phase. Three of the shots had two pellets injected early. The timing can be seen from the traces of the measured central electron densities

in Fig. 2. The numbers of Li ions injected into the last closed flux surface LCFS is calculated in TRANSP using the discontinuities of the measured electron density profiles n_e before and after each pellet. Example of the measured n_e and computed n_{Li} profiles for one of the pellets are shown in Fig. 4. The number of Li ions injected into the LCFS is calculated to be 4×10^{20} . The numbers of Li ions calculated this way for each of the pellets are given in Table I. The number of Li ions is calculated to decrease below 6×10^{17} by 3.7 s, i.e., 300 msec after the start of NBI. For comparison, the maximum number of thermal deuterons within the LCFS (during the NBI phase) is $4\text{-}5 \times 10^{20}$.

The number of Li ions from each pellet is 5×10^{20} , so the TRANSP calculations indicate that most of the injected Li penetrates the LCFS. One source of uncertainty in the TRANSP calculation is the lack of measured Z_{eff} profiles during the Ohmic phases when the pellets are injected. The Z_{eff} profile during the NBI phase used in TRANSP is from the measured carbon density shape normalized by a calibrated visible bremsstrahlung emission measurement.

Density profiles at the end of the NBI are shown in Fig. 5. A slight, but significant decrease in n_e outside of x (defined by the square-root of the toroidal flux) = 0.4 is seen in Fig. 5-a. The measured carbon impurity density n_C increases in the core (Fig. 5-b), but the thermal deuterium density n_D also increases in the core (Fig. 5-c). This is important for increasing the neutron emission rate.

The deposition rates of the beam neutrals depends sensitively on the n_e profile. Profiles of the deposition rates are shown in Fig. 6. The deposition rate in the core more than doubles with conditioning. The electron source rate from ionizations caused by beam injection is shown in Fig. 7-a. The volume-average source rate of electrons in the core ($x < 0.2$) is about $1.4 \times 10^{20}/m^3/s$ for the four shots with $P_{\text{NBI}} = 19$ MW and $2.0 \times 10^{20}/m^3/s$ for the last shot (with $P_{\text{NBI}} = 24.8$ MW.) These rates are 30 % greater than the average rate of increase of n_e shown in Fig. 2 at the start of the beam injection. Thus 70% of the beam ionization rates in the core during the first 300 msec of injection can account for the rise in n_e during that time. For comparison, the estimated rate of ionizations from recycling deuterium is shown in Fig. 7-b.

Heating profiles from the NBI are shown in Fig. 8. The NBI heating of thermal ions in the core is considerably higher than that of (thermal) electrons. Higher rates of ion heating are achieved in the shots with better conditioning. The higher heating results in large central ion temperatures (Fig. 9). The peak values are doubled as a result of the Li pellet conditioning. The peak values for last two shots in the series are among the highest measured in TFTR. The electron temperature profiles (Fig. 9-c) also become more peaked with higher central values. Since the beam-electron heating does not change significantly, the increase is due mainly to increased ion-electron energy transfer.

There are speculations [10] that with sufficient coverage of Li on the walls to prevent recycling the temperature profiles will have reduced gradients in the core and high temperatures near the wall. A benefit of this could be reduced turbulence, high beta, and fusion power. There was no tendency with Li pellet conditioning in TFTR for either T_i or T_e to increase near the edge. This lack of broadening of T_i or T_e could indicate that not enough Li ions were injected in this series to cause this effect.

The toroidal rotation profiles increase with Li pellets. They are shown in Fig. 10. The higher central T_i results in higher total stored energy, and the higher central T_i and n_D result in higher neutron emission. These are shown in Fig. 11. The last shot in the series (76654) had higher P_{NBI} than the others, and the higher heating explains most of the increase above the earlier shots.

Thus Li pellet conditioning in TFTR results in a reduction of the edge density which allowed increased neutral beam penetration, central heating, and fueling. This allows increased peaking of the density and temperature profiles, and higher central T_i , T_e , and neutron emission rates.

This research is supported by the U.S. Department of Energy under contract number DE-AC02-09CH11466.

-
- [1] “The 2nd International Symposium on Lithium Applications for Fusion Devices” (2011) Princeton, http://isla2011.pppl.gov/PPPL%20Li%20Workshop%202011_Abstracts_4-22-11.pdf
- [2] Snipes, J.A.; Granetz, R.S.; Greenwald, M.; Hutchinson, I.H.; Garnier, D.; Goetz, J.A.; Golovato, S.N.; Hubbard, A.; Irby, J.H.; LaBombard, B.; Luke, T.; Marmor, E.S.; Niemczewski, A.; Stek, P.C.; Takase, Y.; Terry, J.L.; Wolfe, S.M., “First ohmic H modes in ALCATOR C-MOD” *Nuclear Fusion*, **3**, (1994) 1039
- [3] Takase, Y.; Boivin, R.L.; Bombarda, P.T.; Bonoli, P.T.; Christensen, C.; Fiore, C.; Garnier, D.; Goetz, J.A.; Golovato, S.N.; Granetz, R.; Greenwald, M.; Horne, S.F.; Hubbard, A.; Hutchinson, I.H.; Irby, J.; LaBombard, B.; Lipschultz, B.; Marmor, E.; May, M.; Mazurenko, A.; McCracken, G.; O’Shea, P.; Porkolab, M.; Reardon, J.; Rice, J.; Rost, C.; Schachter, J.; Snipes, J.A.; Stek, P.; Terry, J.; Watterson, R.; Welch, B.; Wolfe, S., “Radiofrequency-heated enhanced confinement modes in the ALCATOR C-Mod tokamak” *Physics of Plasmas*, **4** 1997 1647.
- [4] Mansfield, D.K, *et al.*, *Nuclear Fusion*, **41**, (2001) 1823.
- [5] Snipes, J.A.; Marmor, E.S., *et al.*, *Jour. Nucl. Materials*, **196-198**, (1991) 686.
- [6] R. V. Budny, *Nucl. Fusion* **34** (1994) 1247.
- [7] Anderson H., *et al.*, *Plasma Physics and Controlled Fusion* **42** (2000) 781.
- [8] Summers H. P., “The ADAS User Manual v2.6”, <http://www.adas.ac.uk/manual.php>
- [9] L. Dectyarev and V. Drozdov, “An inverse variable technique in the MHD-equilibrium Problem”, *Computer Physics Reports* **2**, (1985), 341.
- [10] Krasheninnikov, S.I., Zakharov, L.E., Pereverzev, G.V., *Phys. of Plasmas* **10** (2003), 1678.

Shot number	1st pre-NBI	2nd pre-NBI	NBI	post-NBI
Injection time [s]	2.2	2.7	3.5-4.7	4.8
76649	0	0	19.0	0.1
76650	0	4.5	19.0	3.8
76651	3.2	4.0	19.0	4.9
76653	3.7	1.2	19.0	3.7
76654	3.5	2.3	24.8	3.7

TABLE I: Number of *Li* ions injected within the last closed flux surface [10^{20}] and P_{NBI} [MW]. The number of *Li* ions is derived by TRANSP from the discontinuity in the measured n_e profiles after the injection. The *Li* is computed to exit the last closed flux surface with a half-life of 200 msec.

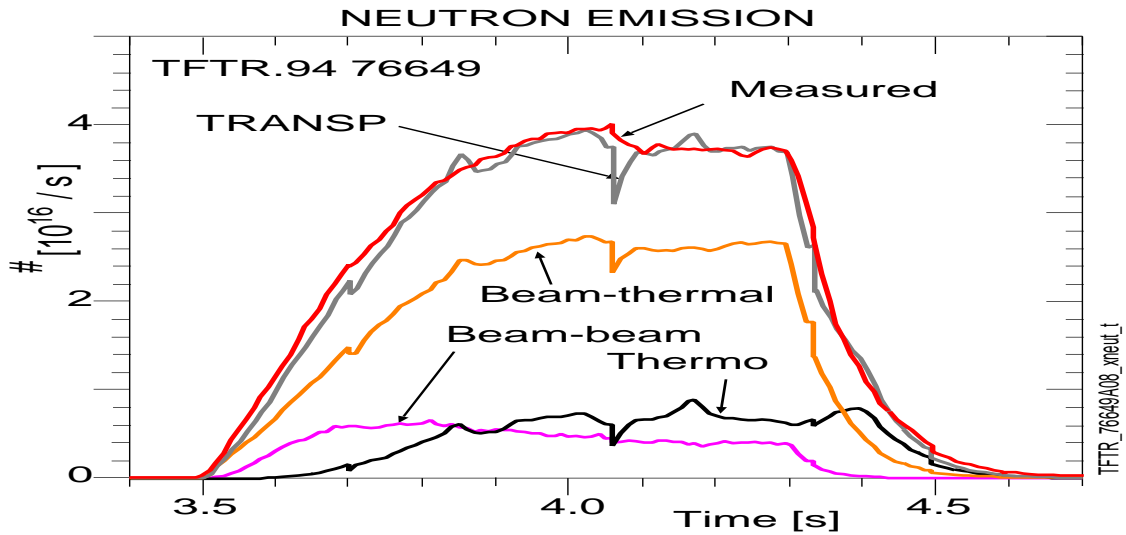


FIG. 1: Measured and computed neutron emission rates for the first (unconditioned) shot of the start of the conditioning series. The approximate agreement between the measured and TRANSP simulated total neutron rate indicates accuracy of the TRANSP analysis.

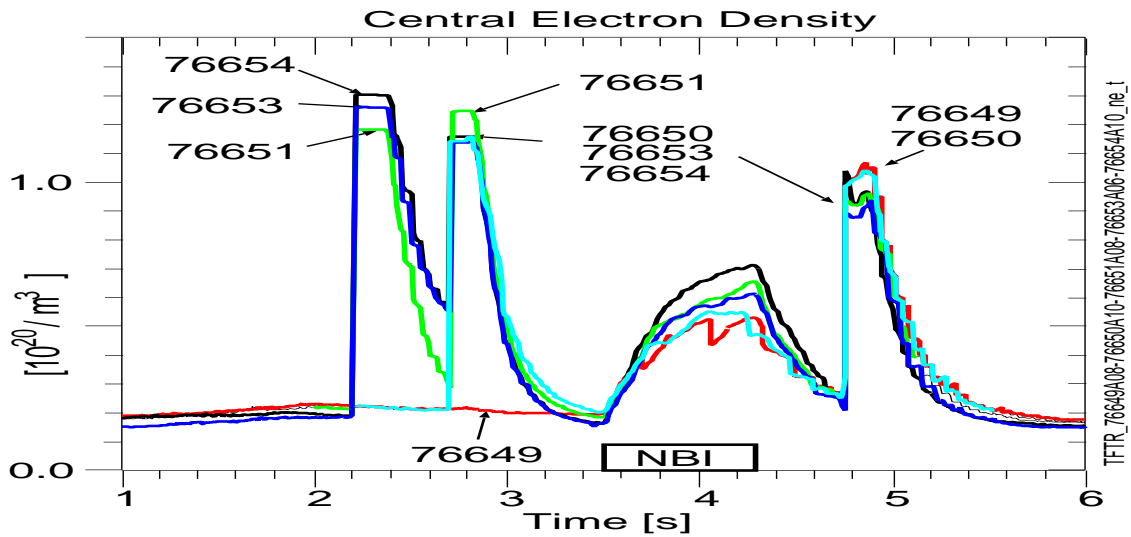


FIG. 2: Central electron densities. One Li pellet was injected into the post-NBI phase of all the shots. One Li pellet was injected into the the pre-NBI phase of the second shot. Two Li pellets were injected into the pre-NBI phase of last three shots. Sawteeth effects are seen in the first shot of the series.

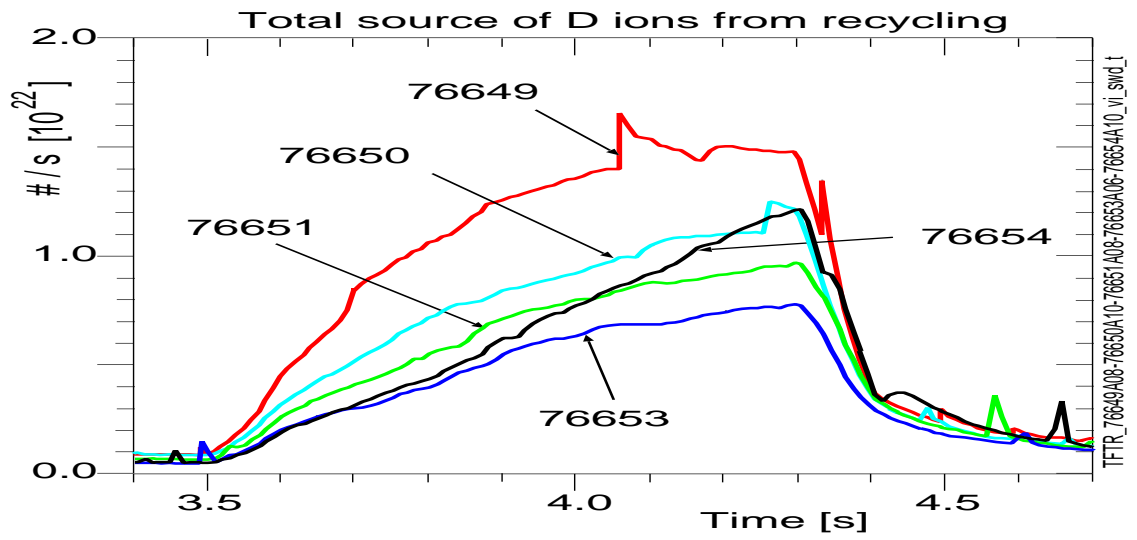


FIG. 3: Rate of ionizations from recycling deuterium calculated from D_{α} emission and scaled by a constant to convert photons to ionizations within the last closed flux surface. The constant is calculated by DEGAS modeling of D_{α} emission along five chords measured in similar plasmas. The rate decreases more than a factor of two with conditioning.

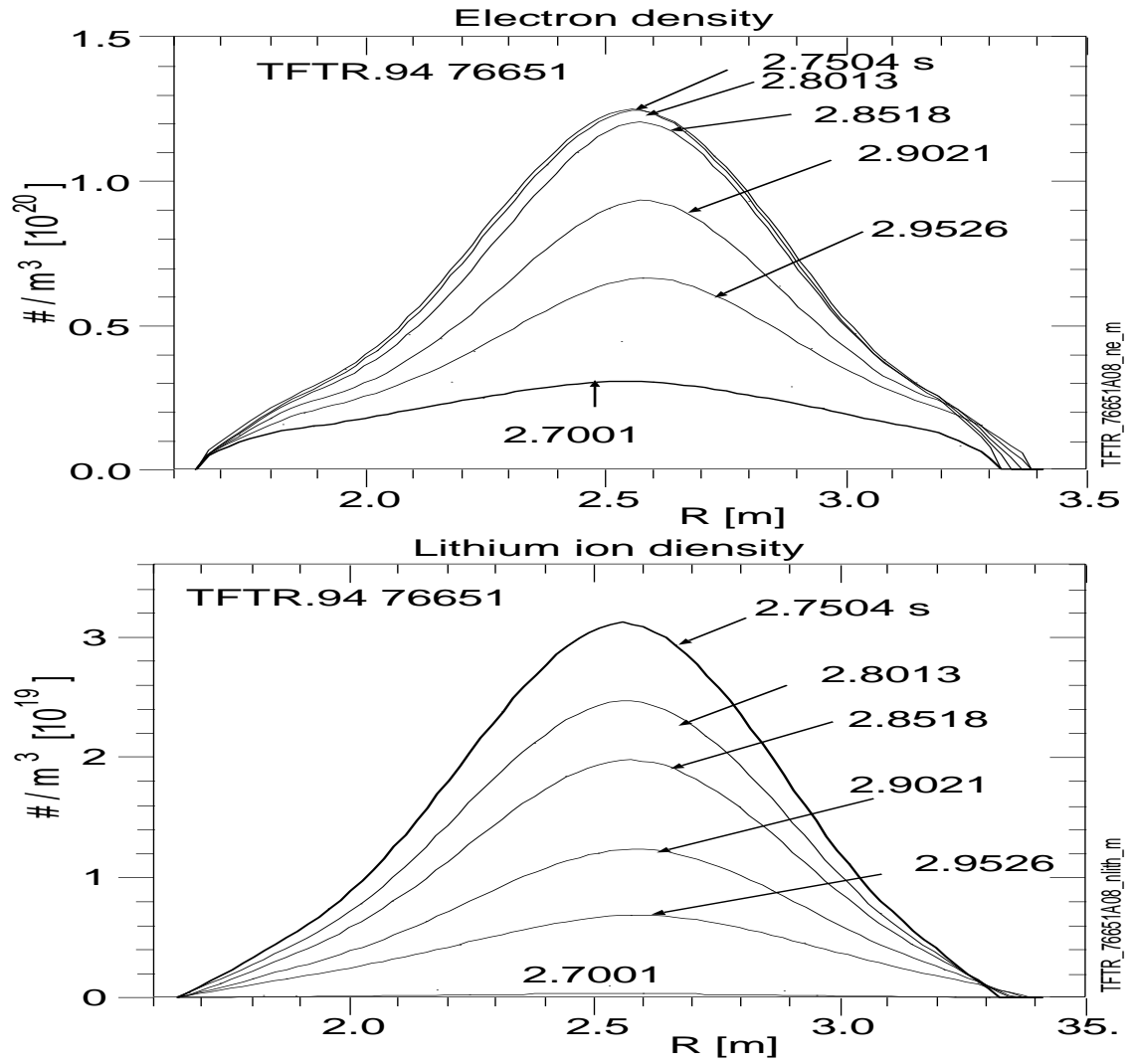


FIG. 4: Measured n_e and computed n_{Li} profiles for the second pre-NBI pellet in the third shot of the conditioning series.

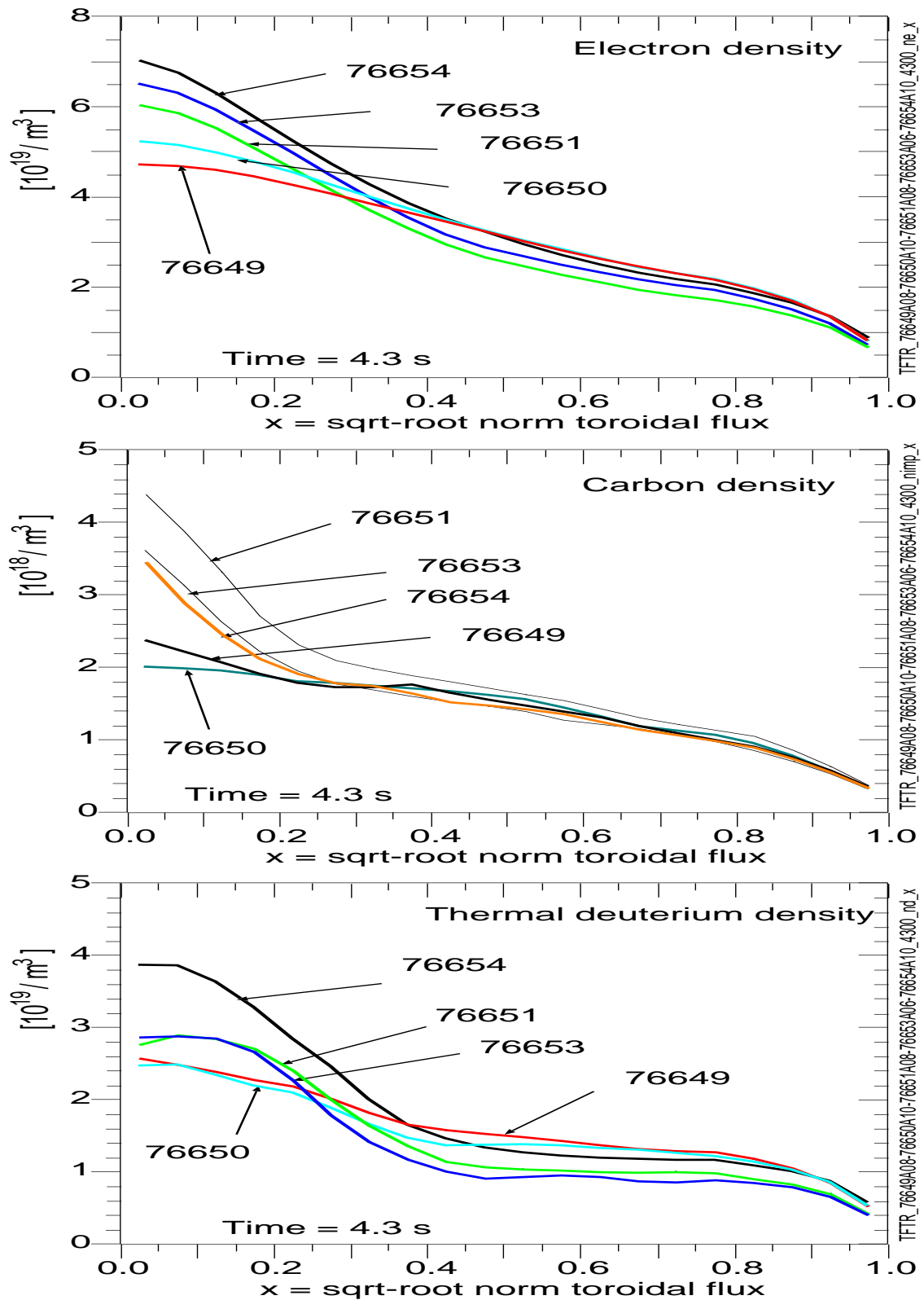


FIG. 5: Electron, carbon impurity, and thermal deuterium densities profiles at 4.3s. The deuterium density is computed in TRANSP by local charge neutrality using the beam and carbon densities.

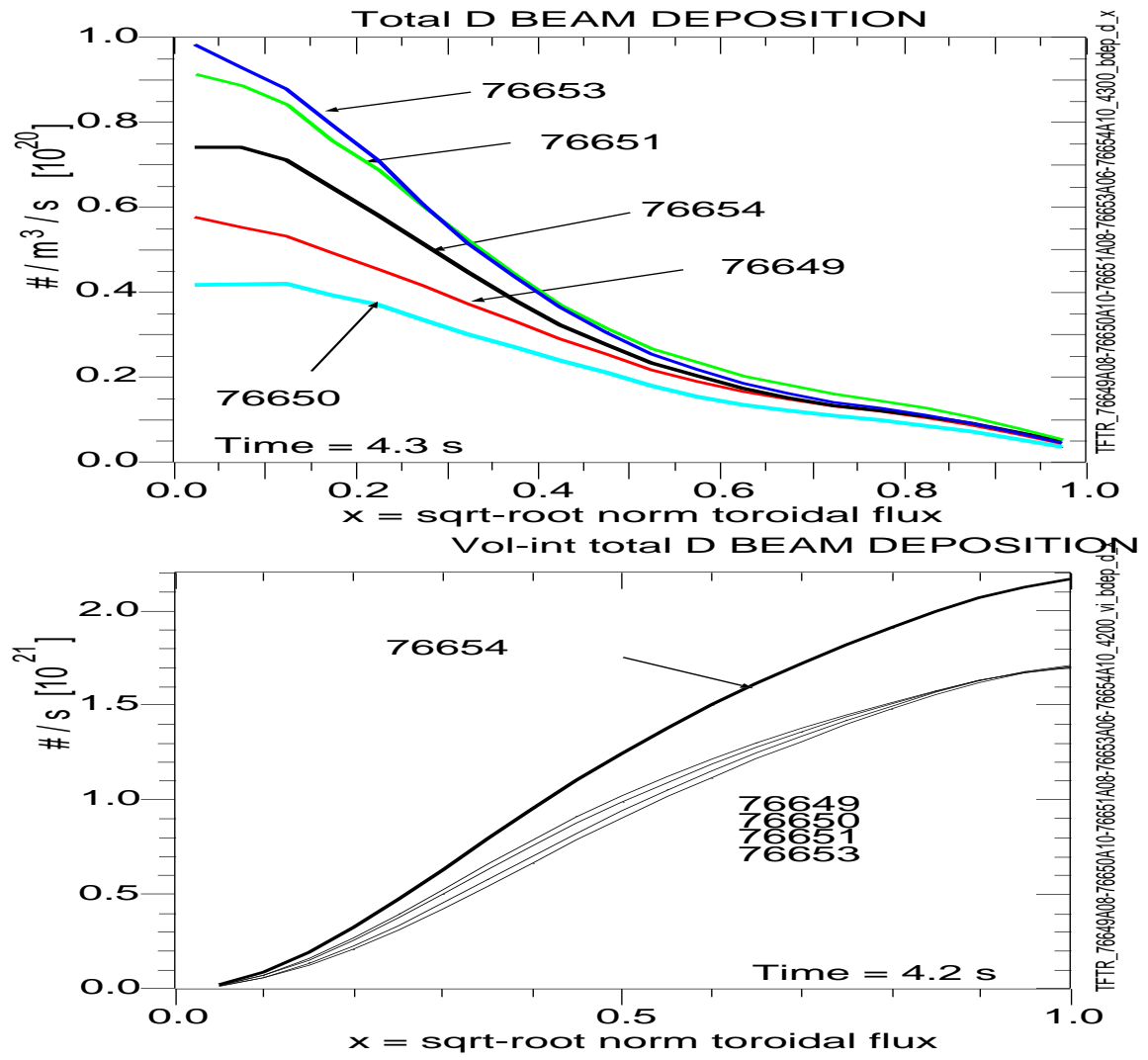


FIG. 6: Profiles of the beam deposition and volume-integrated deposition.

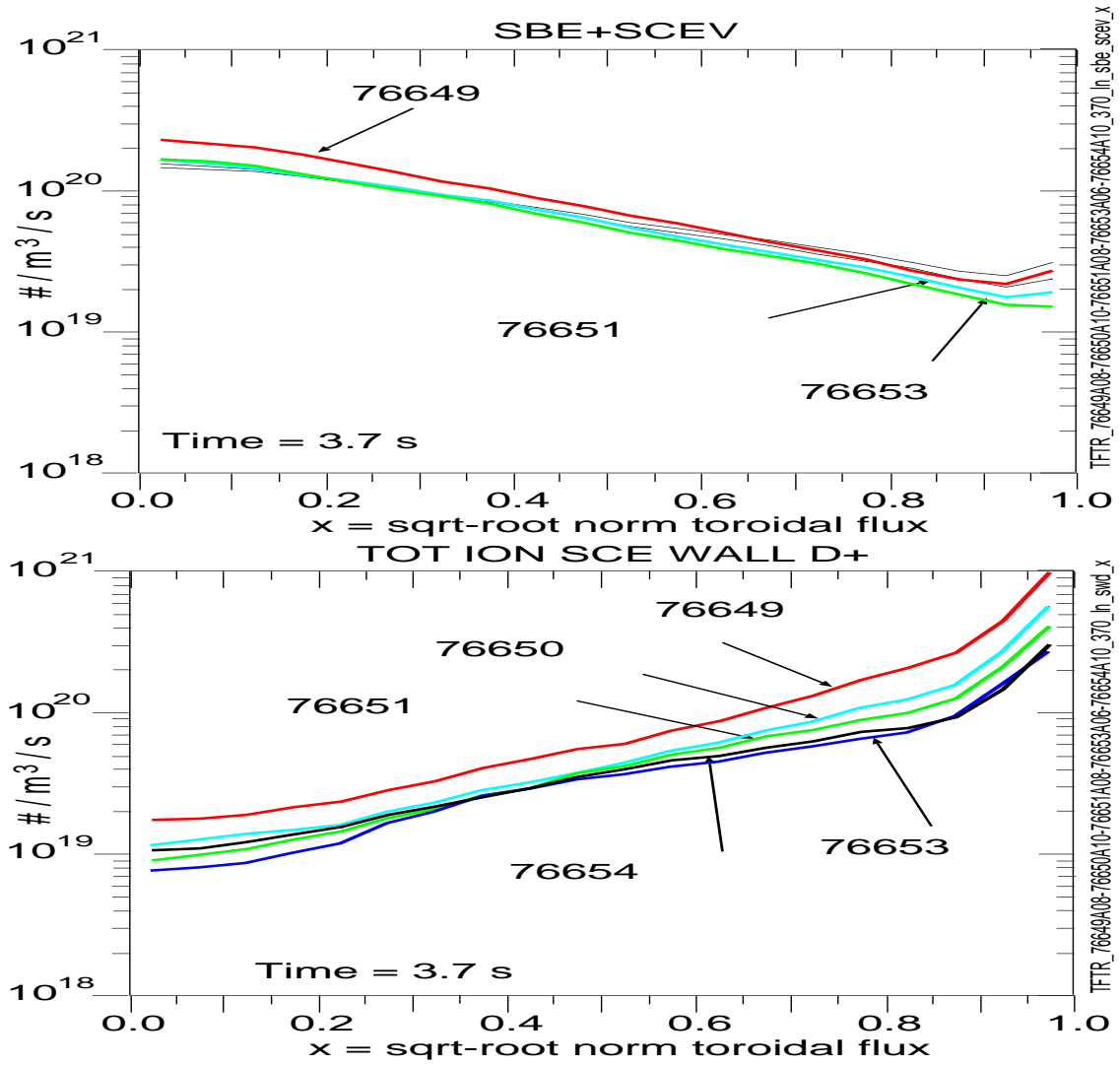


FIG. 7: Profiles at 3.7 s of a) electron ionizations of beam neutrals; b) ionizations of deuterium from wall recycling (inferred from the measured D_α emission and DEGAS modeling); Recycling dominates outside $x = 0.5$ and beam fueling dominates inside.

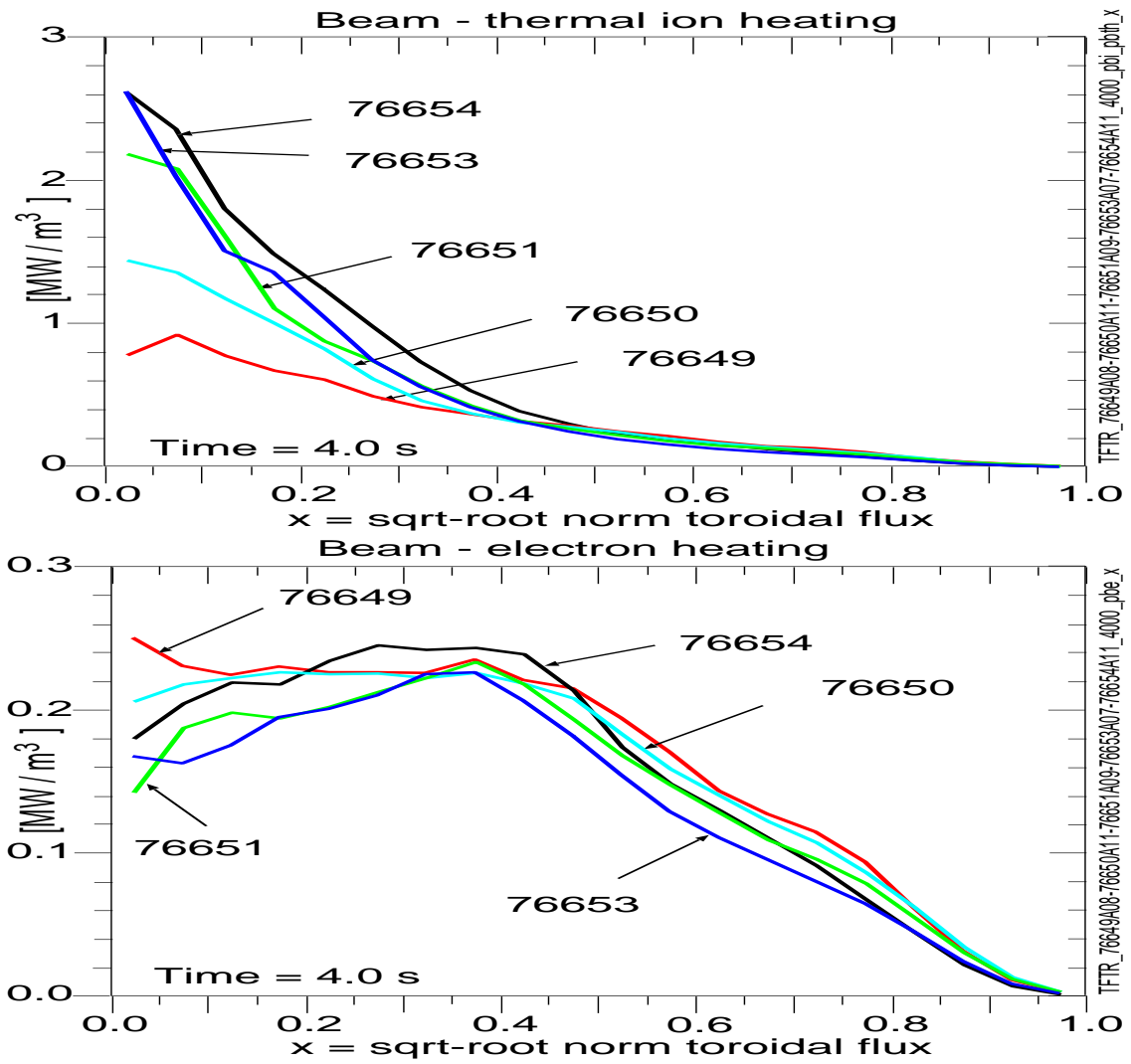


FIG. 8: Profiles at 4.3 of beam heating of a) thermal ions; b) electrons.

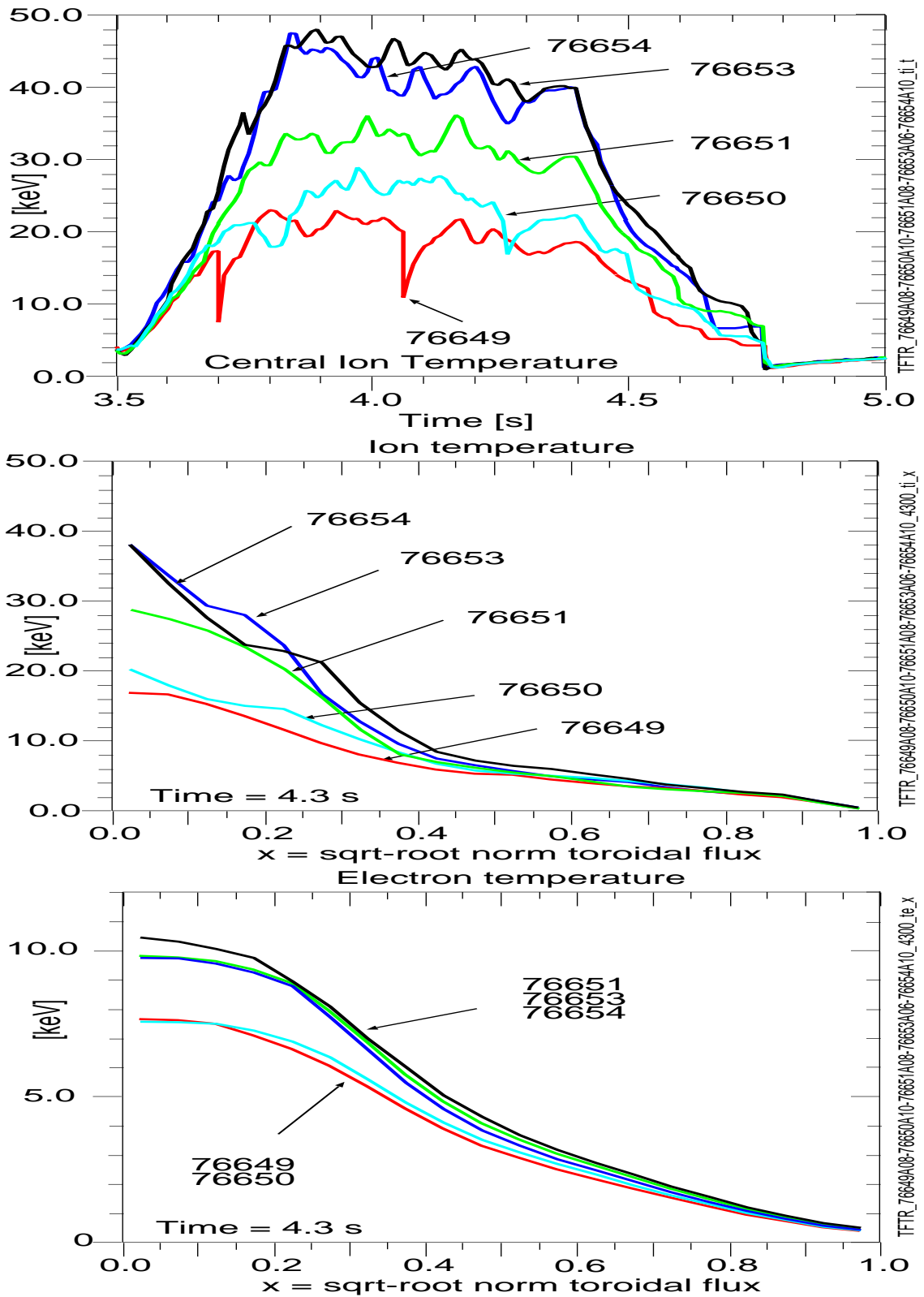


FIG. 9: Ion temperatures a) in the core; b) profiles at 4.3 s.

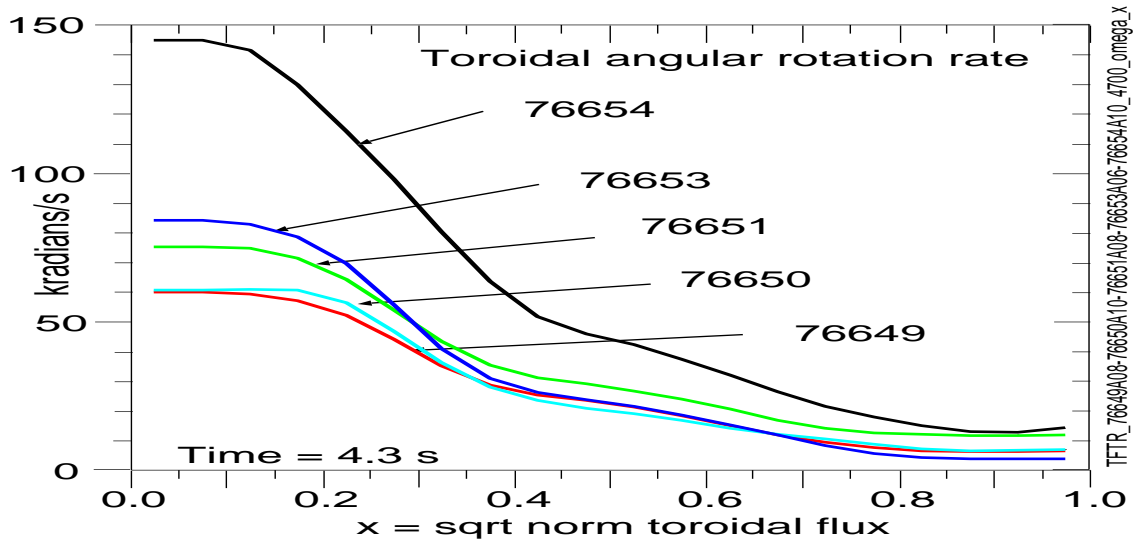


FIG. 10: Ion temperatures a) in the core; b) profiles at 4.3 s.

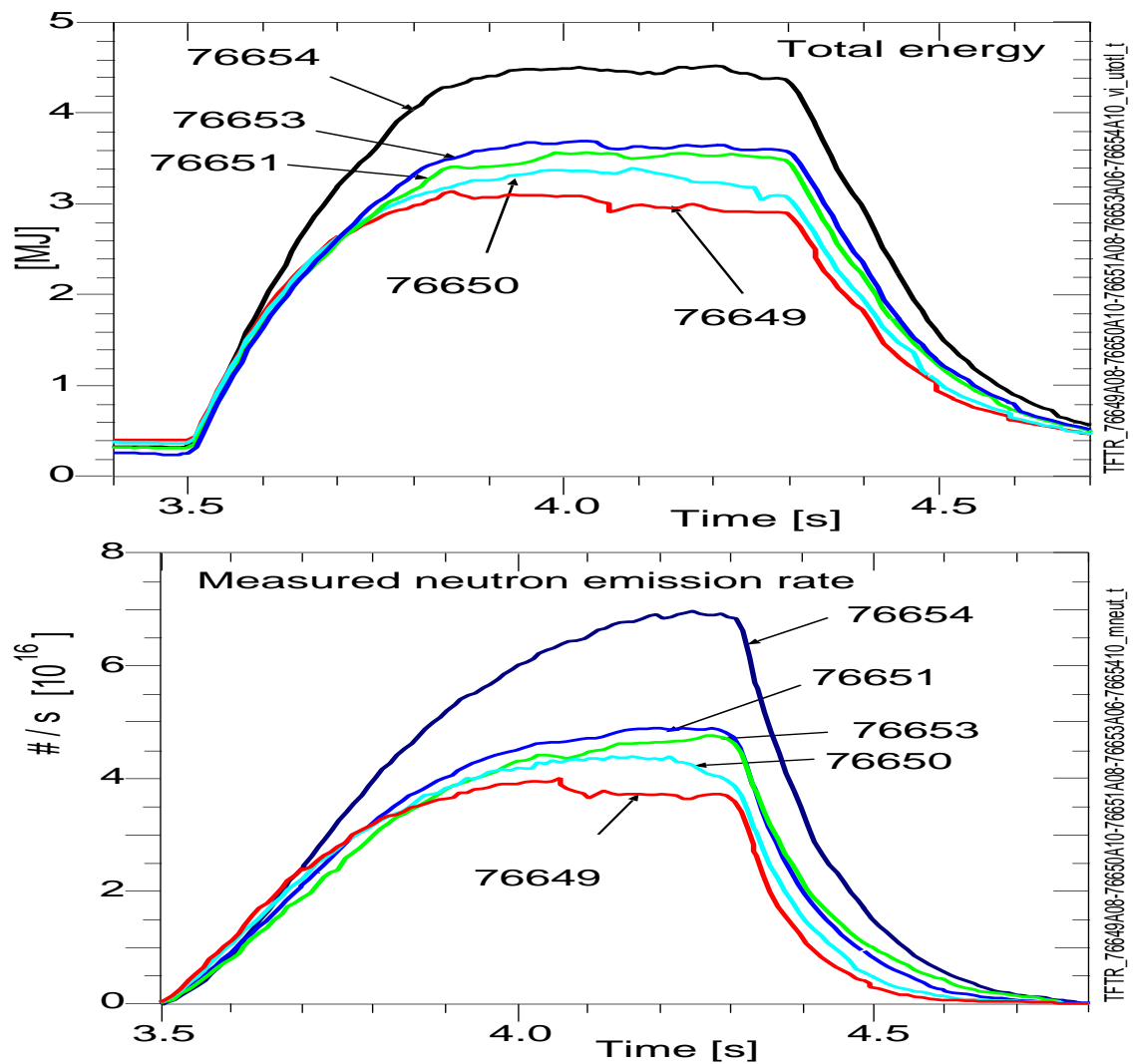


FIG. 11: Total stored energy and measured neutron emission rates.

The Princeton Plasma Physics Laboratory is operated
by Princeton University under contract
with the U.S. Department of Energy.

Information Services
Princeton Plasma Physics Laboratory
P.O. Box 451
Princeton, NJ 08543

Phone: 609-243-2245
Fax: 609-243-2751
e-mail: pppl_info@pppl.gov
Internet Address: <http://www.pppl.gov>